Renormalization Group Limit Cycle for Three-Stranded DNA

Tanmoy Pal,* Poulomi Sadhukhan,† and Somendra M. Bhattacharjee‡

Institute of Physics, Bhubaneswar 751005, India

(Received 23 August 2012; published 11 January 2013)

We show that there exists an Efimov-like three strand DNA bound state at the duplex melting point and it is described by a renormalization group limit cycle. A nonperturbative renormalization group is used to obtain this result in a model involving short range pairing only. Our results suggest that Efimov physics can be tested in polymeric systems.

DOI: 10.1103/PhysRevLett.110.028105 PACS numbers: 87.14.gk, 64.60.ae, 87.15.Zg

Consider a three-particle quantum system with a pairwise short-range potential. Apart from the occurrence of the usual three-body bound state, a very special phenomenon occurs at the critical two-body zero-energy state. An infinite number of three-body bound states appear though the corresponding potential is not appropriate to bind any two of them; the removal of any one of them destroys the bound state. This phenomenon, valid for any short-range interaction, is known as the Efimov effect. The size of the three-body bound states, or Efimov trimers, is large compared to the potential range, and so it is a purely quantum effect [1]. Although it was predicted in the context of nuclear physics [2,3], it has now been detected in cold atoms [4].

An ideal DNA consisting of two Gaussian polymers interacting with native base pairing undergoes a critical melting transition where the two strands get detached. Maji *et al.* recently showed that if, to a double-stranded DNA at its melting point, a third strand is added, the three together would form a bound state instead of remaining critical [5]. The existence of a triplex has further been verified by real space renormalization group (RG) and transfer matrix calculations [5,6]. That this is an Efimov-like effect can be seen by the imaginary time transformation of the quantum problem in the path integral formulation. The paths in quantum mechanics are identified as Gaussian polymers and the equal time interaction maps onto the native base pairing. Such a bound state of a triple-stranded DNA is called an Efimov DNA.

In both cases, the special effect is due to a long-range attraction generated by critical fluctuations at the transition point. For the DNA case, the large fluctuations in the bubble sizes at the melting point allow a third strand to form bound segments with the other two. The power law behavior of the size of a polymer is essential to induce a $1/R^2$ interaction between any two chains [5].

Universal aspects of polymers are well understood in the RG approach [7]. A single chain and many chain solutions are described by length scale dependent running parameters, which, with increasing length scales, are expected to reach certain fixed points. The purpose of this Letter is to show that the triple chain bound state at the duplex melting point is of a different type. This ''few-chain problem'' is actually described by a renormalization group ''limit cycle''[2,8]. The appearance of a limit cycle invokes log periodicity in the corresponding three-body coupling in the polymer problem. So they break the continuous scale invariance around the two-body fixed point imposing a discrete scaling symmetry, the hallmark of the Efimov states.

Another motivation of this Letter is to emphasize that a three-chain polymer model, a three-stranded DNA in particular, by virtue of mathematical similarities, provides an alternative system for Efimov physics. Triplex DNA is known to occur in nature. The possibility of recognizing the bound base pairs of a duplex without opening it, by forming Hoogsteen pairs, has the potentiality of designing new types of antibiotics. In addition, H-DNA is a common motif formed during many DNA activities where there is a stretch of triplex DNA via a strand exchange mechanism [9]. The advantage with our model is that the parameters corresponding to the polymers are easily tunable by changing temperature, solvent conditions, etc. Some important phenomena are getting verified in the mathematically analogous low energy condensed matter systems, e.g., Majorana fermions [10], the Klein paradox [11], and structure formations in the early Universe [12]. We hope that this work will inspire experimental searches of the Efimov effect in polymers.

Because of different critical dimensions of the two-chain and the three-chain interactions, namely, $d = 2$ and $d = 1$, respectively, one has to tackle irrelevant variables in three dimensions, which is outside the scope of the perturbative RG. This makes the problem difficult to handle in traditional Edwards Hamiltonian [7] approach.

Our model consists of three directed polymer chains in $(3 + 1)$ dimensions, where the monomers live in three spatial dimensions ($\mathbf{r}$) and we assign an extra dimension along the contour of a polymer (z). Two polymers can interact only when they are at the same space and length coordinate (native base pairing). To avoid difficulties in solving the full three-chain problem, we consider a simplified model that any two of the three chains are in a bound state. At zero temperature, the two chains form a

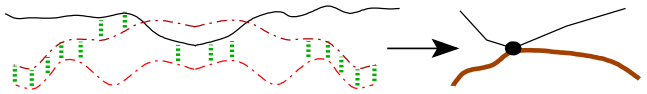

FIG. 1 (color online). Schematic diagram of strand exchange and the equivalent coarse-grained three chain interaction. A single strand (solid black line) pairs with the strands [dash-dot lines (left)] of a bubble on a duplex [thick line (right)]. Short green dotted lines indicate base pairings.

rigid rodlike bound state without any bending. At finite temperature, thermal fluctuation melts locally the bound state to form a number of bubbles, or segments of a free-chain pair, creating interfaces. A weight factor g_2 is given to each interface or Y fork. The bubbles allow the paired bound state to bend. Any unbound chain is taken as free and Gaussian. A bubble of two free chains allows a third chain to pair with one of them (Fig. 1). This is the strand exchange mechanism already alluded to. Such an exchange generates an effective three-chain interaction which, in the presence of large fluctuations in bubbles, creates a triplex bound state at the critical point of the two-chain melting.

Our methodology is to find the two-chain partition function at the melting point and thereafter determine the third virial coefficient for three chains at the duplex melting point. Denoting the dimensionless effective three-chain coupling constant by H, our main result shows that the RG beta function is of the form

$$\Lambda \frac{\partial H}{\partial \Lambda} = -A(H - H_0)(H - H_0^*), \tag{1}$$

where Λ is the inverse of a small length scale cutoff, A is a real constant, and H_0 is a complex number. Because of this pair of complex fixed points there will be a limit cycle behavior, but most importantly, there will be a bound state since $H \to -\infty$.

Figure 2 shows the basic building blocks of the model. To avoid the infinite entropy per unit length of this continuous model, the unconstrained entropy of a single chain is taken as $\ln\mu$ per unit length. For the two-chain bound state, we assign an energy $\propto \epsilon(<0)$ per unit length. We take $k_BT = 1$, where k_B is the Boltzmann factor and T is the temperature. The free chain and the bound state partition functions for chain length N and end-to-end distance $\mathbf{r}$ are given, respectively, by [13]

$$\mathsf{Z}(\mathbf{r}, N) = \mu^{N\Lambda^2}(2\pi N)^{-d/2} e^{-(\mathbf{r}^2/2N)}, \tag{2a}$$

and

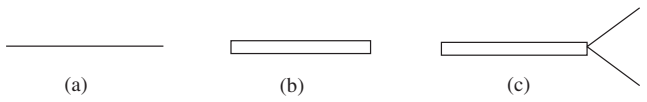

FIG. 2. Basic building blocks. (a) represents $Z(\mathbf{k}, s)$ for a Gaussian chain, (b) $Z_b(\mathbf{k}, s)$ for a two chain bound state, (c) a Y fork representing the interface between a bound pair and two open strands. It has a weight g_2.

$$\mathsf{Z}_\mathsf{b}(\mathbf{r}, N) = e^{-\epsilon N\Lambda^2}(4\pi)^{-1}\delta(\mathbf{r} - N\Lambda\hat{\mathbf{n}}), \tag{2b}$$

where $\hat{\mathbf{n}}$ is a unit vector, giving the direction of the rigid rod. It is convenient to work in the Fourier-Laplace $(\mathbf{k}, s)$ space, where $\mathbf{k}$ and s are Fourier and Laplace conjugates of $\mathbf{r}$ and N, respectively. In $(\mathbf{k}, s)$ space the above partition functions read [14]

$$Z(\mathbf{k}, s) = (s - \Lambda^2 \log\mu + k^2/2)^{-1}, \tag{3a}$$

$$Z_\mathsf{b}(\mathbf{k}, s) = \frac{1}{k\Lambda}\arctan\frac{k\Lambda}{s + \epsilon\Lambda^2} \overset{k\to 0}{=} \frac{1}{s + \epsilon\Lambda^2}. \tag{3b}$$

The Gaussian behavior is reflected in the average size as measured by the mean squared distance $\langle r^2\rangle \sim N$. The poles in s of Eqs. (3a) and (3b) for $k = 0$ at $\Lambda^2\log\mu$ and $-\epsilon\Lambda^2$ are the negative free energies of a free chain and a bound pair respectively. Here $\mathbf{k} = 0$ corresponds to the free-end eensemble case. For simplicity, the $k \to 0$ form of Z_b could be used.

As our partition functions are translationally invariant and a forking can take place at any s, we have $\mathbf{k}$, s conservation at each vertex point. As arbitrary number of bubbles are allowed, the finite temperature bound state partition function can be written as an infinite geometric series as shown in Fig. 3(a). We name the black box on the left-hand side as a *duplex*. The duplex partition function, obtained by summing the infinite series, is given by

$$Z_d(\mathbf{k}, s) = Z_b(\mathbf{k}, s)[1 - g_2^2 I_0 Z_b(\mathbf{k}, s)]^{-1}. \tag{4}$$

Here the single bubble contribution I_0 is [15]

$$I_0 = 4\pi\Lambda - 2\pi^2\sqrt{s' + k^2/4}, \tag{5}$$

in the limit $(s' + k^2/4) \to 0$ where $s' = s - 2\Lambda^2\log\mu$.

We want to concentrate on the events near melting where bubbles proliferate. For $s', k \to 0$, we find the singularity of Z_d to be

$$\sqrt{s'_*} = -(2\pi^2)^{-1} g_2^{-2}\Lambda^2\Delta t, \tag{6}$$

where $\Delta t \equiv 2\log\mu + \epsilon - 4\pi g_2^2\Lambda^{-1}$ is the deviation from the duplex melting point with the melting transition at $\Delta t = 0$ [16]. The singularity s'_* is the free energy difference of the duplex and two unbound chains. We choose g_2 as the tuning parameter to get melting. The usual scaling

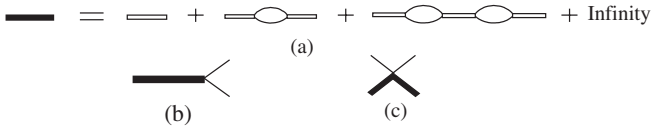

FIG. 3. (a) The duplex partition function as an infinite series of bound pairs and bubbles; (b) Y fork for a duplex. (c) A three chain interaction, g_3, involving a free chain and a duplex.

for ideal DNA melting can also be recovered from Eq. (6), viz.,

$$s'_* \sim \xi^{-2}, \quad \text{with} \quad \xi \sim |\Delta t|^{-1}. \tag{7}$$

Here, ξ is a diverging length scale for this continuous melting. In the absence of g_2 the denaturation transition is first order with $s = -\epsilon\Lambda^2$ and $s = 2\Lambda^2 \ln\mu$ for the bound and the free phases, respectively.

When the system length scale ξ diverges for some critical value of g_2 the system goes to the stable free chain phase. The full duplex partition function can now be written in terms of ξ in the small s' limit as

$$Z_{\mathrm{d}}(\mathbf{k}, s) = \left(2\pi^2 g_2^2\left[-\xi^{-1} + \sqrt{s' + k^2/4}\right]\right)^{-1}. \tag{8}$$

The two-chain melting behavior is similar to the necklace model [17]. We note two features. First, there is a diverging length scale $\xi \sim |\Delta t|^{-1}$. Second, under a scale change $\mathbf{k} \to b^{-1}\mathbf{k}$, the length scale and the free energy change as $\xi \to b\xi$ and $f \to b^{-2}f$, respectively, for any arbitrary b. This is continuous scale invariance.

Now, let us consider the three-chain case where two of them are in the duplex state and the third is free. In the presence of bubbles we replace Fig. 2(c) by Fig. 3(b) and call it as our two-chain coupling g_2. A duplex can dissociate into two free chains and if one of them interacts with the third free chain they can again form a duplex. As a duplex can bend thanks to the presence of bubbles we can also have diagram like Fig. 3(c). This is our three-chain coupling g_3. The free-chain-duplex interaction vertex, W, is the third virial coefficient which comes from all the three-chain connected diagrams as shown in Fig. 4. The purpose of introducing the three-chain interaction is to make the virial coefficient independent of the arbitrary cutoff. This can be achieved by doing a momentum shell type integration over a thin shell which will also give the beta function for the three chain interaction.

Translational invariance suggests that the partition function depends only on the duplex-single chain separation at the two end points. The total momenta at each end can therefore be taken to be zero. The evaluation of diagrams of Fig. 4 gives

$$W(\mathbf{k}, \mathbf{k}', s_1, s'_1, s) = 2g_2^2 Z(\mathbf{k} + \mathbf{k}', s - s_1 - s'_1) + g_3 + (2\pi i)^{-1}\int d\mathbf{q}\, d\bar{s}(2g_2^2 \mathcal{I}_1 + g_3 \mathcal{I}_2), \tag{9}$$

where,

FIG. 4. Diagrammatic representation of the three chain partition function. This translates into an integral equation involving interactions to all order.

$$\mathcal{I}_1 = Z(\mathbf{q}, \bar{s})Z(\mathbf{k} + \mathbf{q}, s - s_1 - \bar{s}) \times Z_{\mathrm{d}}(-\mathbf{q}, s - \bar{s})W(\mathbf{q}, \mathbf{k}', \bar{s}, s'_1, s), \tag{10}$$

and,

$$\mathcal{I}_2 = Z(\mathbf{q}, \bar{s})Z_{\mathrm{d}}(-\mathbf{q}, s - \bar{s})W(\mathbf{q}, \mathbf{k}', \bar{s}, s'_1, s). \tag{11}$$

We further simplify our model by averaging over all angles and assuming the external free chains are in relaxed state such that (s_1, k) and s'_1, k' satisfy the pole condition of Eq. (3a) [18]. Near melting, $s - 3\Lambda^2 \log\mu$ is very small for three chains, and, $\xi \to \infty$. So most of the contribution comes from the loop diagrams. Neglecting the tree level contributions [19], we have

$$\overline{W}(k) = \frac{8}{\sqrt{3}\pi}\int_0^\Lambda dq\left[\frac{1}{q}\log\frac{k^2 + q^2 + kq}{k^2 + q^2 - kq} + 2k\frac{H(\Lambda)}{\Lambda^2}\right]\overline{W}(q), \tag{12}$$

in terms of the redefined dimensionless quantities

$$\overline{W}(q) = qW(q), \quad \text{and} \quad H(\Lambda) = \Lambda^2 g_3 (2g_2)^{-2}, \tag{13}$$

For $H = 0$, there is no scale in the limit $\Lambda \to \infty$, and Eq. (12) has a solution

$$\overline{W}(k) = C\cos[s_0 \log(k/\Lambda_*)], \tag{14}$$

where C, Λ_* are constants and $s_0 = 1.5036$. When $H \neq 0$ and Λ is finite we can still use this solution as it retains its form changing only its constants [20].

We now use a momentum shell technique to get the behavior of $H(\Lambda)$. We first integrate over a small shell of radius $\Lambda e^{-\mathrm{dl}}$ in Eq. (12) and then rescale back $\Lambda \to \Lambda e^{\mathrm{dl}}$ to get the following differential equation in the limit $k \ll \Lambda$,

$$\frac{1}{\Lambda}\left[\Lambda\frac{\partial H}{\partial \Lambda} - 2H\right]\int_0^\Lambda \overline{W}(q)dq + [1 + H]\overline{W}(\Lambda) = 0. \tag{15}$$

Using the form of $\overline{W}$ of Eq. (14), we have the solution

$$H(\Lambda) = -\frac{\sin\left[s_0 \log\frac{\Lambda}{\Lambda_*} - \arctan(\frac{1}{s_0})\right]}{\sin\left[s_0 \log\frac{\Lambda}{\Lambda_*} + \arctan(\frac{1}{s_0})\right]}. \tag{16}$$

Equations (15) and (16) can be combined to obtain the RG flow equation of H as given in Eq. (1) with

$$A = (1 + s_0^2)/2, \quad \text{and} \quad H_0 = (1 + is_0)/(1 - is_0). \tag{17}$$

If we define a new coupling constant $\zeta = (H - H_0)/(H - H_0^*)$, its flow gives limit cycle trajectories [21]. The Λ-independence of H and its log-periodicity for large values of Λ can easily be verified from Eq. (16). As $g_2 =$ const at the two-chain critical point, g_3 satisfies Eqs. (17) and (16), respectively. At the points $\Lambda_n \sim \Lambda_*(e^{\pi/s})^n$, where n's are integers, g_3 runs into negative infinity as Λ is changed [22]. As g_3 can be interpreted as three-chain binding energy, we get Efimov states at these points. When Λ is increased, g_3 continuously decreases to

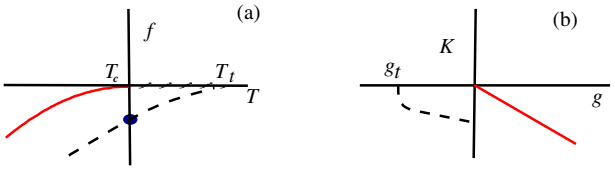

FIG. 5 (color online). (a) Schematic plot of f vs, T. The solid red (dashed black) line is the free energy curve for the duplex (triplex) measured from the unbound state. The continuous melting is at $T = T_c$. The closed circle is the triplex bound state at T_c. The triplex melting at T_t is first order. (b) The corresponding Efimov plot in the K-g plane with line types as in (a).

negative infinity and then jumps to positive infinity in a log periodic manner. Every jump corresponds to a winding around the limit cycle or from one Efimov bound state to other. These states are concentrated at the origin and infinite in number.

So far as the DNA is concerned, the two-chain melting has a critical behavior with free energy given by $f \sim -|T - T_c|^2$ for $T \to T_c -$, measured from the unbound state. The spatial length scale ξ, coming from the fluctuations in the bubble sizes, diverges as given by Eq. (7). However, the addition of an extra similar strand, destroys the continuous scale invariance mentioned below Eq. (8). Instead of three critical pairs, one gets a fluctuation induced bound state with a characteristic length scale Λ_*. By using the quantum path integral to polymer mapping, the DNA partition function can be written as $Z(N) \sim \sum_n \exp(-E_0 \Lambda_n^2 N)$, where E_0 is the ground state energy determined by Λ_*, in units such that $E_0 N \Lambda_*^2$ is dimensionless. We assume that the coefficients do not depend too sensitively on n. For $N \to \infty$, the thermodynamics is determined by the ground state energy E_0. If f and f_N represent the free energy per unit length in the long length limit and for finite length N, then one sees that

$$f = f_N - N^{-1} \ln[1 - \exp(-aNf_{aN} + Nf_n)], \qquad (18)$$

valid only for $a = \exp(2\pi/s_0)$.

Figure 5 shows the equivalence of the free energy curve and the conventional Efimov plot in QM. The filled circle at T_c is the schematic three-chain bound state free energy. The bound state of size Λ_*^{-1}, much larger than the hydrogen bond length would melt at a higher temperature at $T = T_t$. This free energy curve meets the unbound curve at a finite slope indicating a first order transition [5]. The Efimov DNA is observable in the hatched region between T_c and T_t. The equivalent plot for the Efimov case is shown in (b). The ground state energy in QM corresponds to the DNA free energy so that in the Efimov plot, the y axis of the wave number (K) in QM becomes $\text{sign}(f)\sqrt{|f|}$ while the x axis is the temperature deviation from the melting point written in terms of the inverse duplex length scale, $g = \text{sign}(T_c - T)\xi^{-1}$. One recovers the square-root behavior of the trimer energy as it approaches zero and the duplex curve is becoming straight line—familiar from the Efimov plot.

This Letter presents an example of the Efimov effect which is more amenable to experimental verification. Here we show that there exists a triplex state at the critical point of duplex melting of DNA. The derivation uses the nonperturbative RG of a model involving a short-range pairing only. We start from a zero temperature, or, completely bound two-stranded DNA. At nonzero temperature, bubbles form in the bound state and a third strand can form a duplex with any one of the denatured pair or both. The renormalization of the short-range pairing generates an effective three-chain interaction which is responsible for the three-chain bound state. As a result, at the critical point of two-chain melting, there exists a three-chain bound state, but no two-chain bound state. The parameters in the case of polymers are easily tunable, and, therefore, it will be more helpful in detecting the Efimov effect experimentally.

We thank an anonymous referee for a suggestion on the k-dependence in Eq. (3b).

*tanmoyp@iopb.res.in
†poulomi@iopb.res.in
‡somen@iopb.res.in

[1] V. Efimov, Phys. Lett. **33B**, 563 (1970); Sov. J. Nucl. Phys. **10**, 62 (1970); **12**, 1080 (1971).
[2] E. Brateen and H. W. Hammer, Phys. Rep. **428**, 259 (2006).
[3] A. Fonseca, E. Redish, and P. E. Shanley, Nucl. Phys. **A320**, 273 (1979).
[4] S. Knoop, F. Ferlaino, M. Mark, M. Berninger, H. Schöbel, H. C. Nägerl, and R. Grimm, Nat. Phys. **5**, 227 (2009).
[5] J. Maji, S. M. Bhattacharjee, F. Seno, and A. Trovato, New J. Phys. **12**, 083057 (2010).
[6] J. Maji and S. M. Bhattacharjee, Phys. Rev. E **86**, 041147 (2012).
[7] Y. Oono, in *Advances in Chemical Physics*, edited by I. Prigogine and S. A. Rice (Wiley, New York, 1985), Vol. LXI.
[8] S. D. Glazek and K. G. Wilson, Phys. Rev. D **48**, 5863 (1993); Phys. Rev. Lett. **89**, 230401 (2002).
[9] M. D. Frank-Kamenetskii and S. M. Mirkin, Annu. Rev. Biochem. **64**, 65 (1995).
[10] Majorana fermions were detected at the topological insulator superconductor junction. See, e.g., L. Fu and C. L. Kane, Phys. Rev. Lett. **100**, 096407 (2008); V. Mourik, K. Zuo, S. M. Frolov, S. R. Plissard, E. P. A. M. Bakkers, and L. P. Kouwenhoven, Science **336**, 1003 (2012).
[11] The Klein paradox of relativistic quantum mechanics got verified in graphene. See, e.g., M. I. Katsnelson, K. S. Novoslev, and A. K. Geim, Nat. Phys. **2**, 620 (2006).
[12] The Kibble-Zurek model of structure formation in early universe was verified quantitatively in liquid crystals. See, e.g., M. J. Bowick, L. Chandar, E. A. Schiff, and A. M.

Srivastava, Science **263**, 943 (1994); S. Digal, R. Ray, and A. M. Srivastava, Phys. Rev. Lett. **83**, 5030 (1999).

[13] By denoting the dimension of length by L, our choice requires $[\Lambda] = L^{-1}$, $[r] = [k]^{-1} = L$, $[N] = [s]^{-1} = L^2$. Appropriate powers of Λ are used to make various quantities dimensionless. The Fourier transform variable $\mathbf{k}$ will be called "momentum" as per common usage.

[14] For the bound case, in addition to the integral over $\mathbf{r}$ for Fourier transforms, integrations over the angular variables for $\hat{\mathbf{n}}$ are needed.

[15] I_0 is given by $I_0 = \int_{\mathbf{q},\bar{s}} \frac{d\bar{s}}{2\pi i} Z(\frac{\mathbf{k}}{2} - \mathbf{q}, \bar{s}) Z(\frac{\mathbf{k}}{2} + \mathbf{q}, s - \bar{s}) d\mathbf{q}$, which can be evaluated using Eq. (3a) exactly to be $I_0 = 4\pi[\Lambda - \sqrt{s' + k^2/4}\tan^{-1}(\Lambda/\sqrt{s' + k^2/4})]$. Equation (5) can be obtained in the proper limit.

[16] The expression for Δt can be written in a general form as $\Delta t = [Z_b^{-1}(s' \to 0, \mathbf{k} \to 0) - 4\pi g_2^2 \Lambda]\Lambda^{-2}$.

[17] M. E. Fisher, J. Stat. Phys. **34**, 667 (1984).

[18] The pole condition of Eq. (3a) is the free energy relation $s = \Lambda^2 \log\mu - k^2/2$ for a relaxed chain, which is consistent with $r^2 \sim N$ for a Gaussian chain.

[19] The angle averaged partition function from Eq. (9) is $W(k,k') = g_2^2 L(s'', k, k') + g_3 + 4\pi \int_0^\Lambda dq q^2 [2g_2^2 L(s'', k, q) + g_3] Z_{\mathrm{d}}(-q, s + q^2/2) W(k, q)$, where $L(a,b,c) = \frac{1}{bc} \times \log\frac{a+b^2+c^2+bc}{a+b^2+c^2-bc}$, and $s'' = s - 3\Lambda^2 \log\mu$.

[20] P. F. Bedaque, H. W. Hammer, and U. van Klock, Nucl. Phys. **A646**, 444 (1999).

[21] E. B. Kolomeisky and J. P. Straley, Phys. Rev. B **46**, 12 664 (1992); S. Mukherji and S. M. Bhattacharjee, Phys. Rev. E **63**, 051103 (2001).

[22] Λ_n's are given by $\Lambda_n = \Lambda_*(e^{\pi/s_0})^n \exp\left[\frac{\arctan(s_0) - \frac{\pi}{2}}{s_0}\right]$. For the quantum problem, one then gets the characteristic Efimov tower $E_{n+1}/E_n = \text{const}$, where E_n is the three particle energy in the nth state [1].